Journal of Thermal Biology 80 (2019) 94–105

Contents lists available at ScienceDirect

Journal of Thermal Biology

journal homepage: www.elsevier.com/locate/jtherbio

Relationship between metabolic rate and blood perfusion under Fanger thermal comfort conditions

Jure Marn[a], Mo Chung[b,*], Jurij Iljaž[a]

[a] Faculty of Mechanical Engineering, University of Maribor, 2000, Slovenia
[b] Department of Mechanical Engineering, Yeungnam University, Gyeongsan 38541, Republic of Korea

ARTICLE INFO

Keywords:
Fanger thermal comfort
Pennes bioheat equation
Blood perfusion
Temperature distribution
Asymptotic solution

ABSTRACT

The one-dimensional steady Pennes (bioheat) equation was applied to analyze heat conduction inside a combined layer of human muscle and fat, under Fanger thermal comfort conditions. The bioheat equation was solved subject to two boundary conditions at the skin surface: a prescribed skin temperature satisfying the Fanger comfort criterion, and a prescribed heat flux obtained from the overall energy balance for the system. In addition to a fixed body core temperature, an adiabatic condition was imposed as an auxiliary condition at the core of the body, and a pair of equations were derived, relating the blood perfusion and the volumetric heat generation rate for a given activity level and environmental conditions. By solving the two equations, we determined the functional dependence of blood perfusion and metabolic heat generation on the human activity level. For convenience, we presented simple explicit expressions for the key relations, with the aid of asymptotic analyses. Additional results include the temperature distribution inside the muscle layer, and the effects of muscle and fat layer thickness on the heat transfer processes.

1. Introduction

Thermal comfort is largely considered a psychological state that depends on the psychology of an individual in response to the conditions of the environment (Mitchell and Braun, 2012). In many air conditioning design problems, correlations based on experimental results from statistical voting are used to provide most widely acceptable environmental conditions via air conditioning equipment. It is clear that the human perception of thermal comfort is directly linked to the physical variables of the environment, such as the temperature and humidity of the air. In general, human bodies are at a condition where they perceive a certain degree of discomfort due to an inappropriate combination of environmental conditions (such as air temperature and humidity) and heat transfer resistance (clothing). The focus of this study is the consideration of a neutral condition known as *thermal comfort*, as proposed by Fanger (1970). This condition is an ideal condition and serves as the design goal of air conditioning systems.

In this study, we focus our attention only to a system of a human body that is already in the comfort conditions. This means that we are solving a steady state problem without considering the dynamic communications of thermal signals and thermoregulatory mechanisms. The states are special equilibrium states a human body would like to stay depending on the specific activity level of the individual. There are several reasons why a deeper understanding of this particular state is important. As a general rule, when a system is in operation around an equilibrium condition, detailed information for the equilibrium condition itself is useful in many cases. Furthermore, the Fanger thermal comfort criteria are the de facto model adopted by virtually every standard in the world at the moment (ASHRAE, 2009; ISO, 7730, 2005). Heat transfer problems under thermally comfortable conditions should constitute one of the fundamental heat transfer problems in our body because our body spends a substantial amount of time under comfort conditions during our lifetime. Even when we study cases where our body deviates from the equilibrium, the comfortability conditions still serve as a baseline state.

Fanger performed experiments on the human perception of thermal comfort and found that the sensation of thermal comfort was most significantly determined by narrow ranges of skin temperature and sweat evaporation rate, depending on activity level. The comfortability conditions are then derived by correlating the results of psychological experiments to thermal analysis variables (Fanger, 1970). One important observation is that he measured only physical quantities that are easily obtainable by simple experiments. Also, notice that the data is associated with the exterior of the human body. Fanger's model includes the effects of air temperatures and surface temperatures, different humidity, and different airflow velocities. All of them are

* Corresponding author.
E-mail address: mchung@yu.ac.kr (M. Chung).

https://doi.org/10.1016/j.jtherbio.2019.01.002
Received 1 June 2018; Received in revised form 4 January 2019; Accepted 4 January 2019
Available online 07 January 2019

Nomenclature

A_{Du}	DuBois Area [m^2]
c	specific heat [J/kg ℃]
$\bar{E}_s$	energy loss by sweat secretion [W], Eq. (21)
h	specific enthalpy [J/kg]
k	thermal conductivity [W/m ℃]
L_{fat}	fat thickness [m]
L_m	muscle thickness [m]
$\dot{L}$	dry respiration heat loss [W]
m	$\sqrt{\omega\rho_b c_b/k_m}$ [/m]
$\dot{m}_a$	mass flow rate of dry air [kg/s]
$\dot{m}_v$	mass flow rate of water vapor [kg/s]
$\dot{m}_f$	mass flow rate of liquid water [kg/s]
$\dot{M}$	metabolic energy generation [W]
P_{ref}	reference pressure [kPa], Eq. (17)
P_{sat}	saturation pressure of water [kPa]
P_v	partial pressure of the water vapor [kPa]
ΔP_v	$P_v - P_{ref}$ [kPa]
$\dot{q}_m$	volumetric heat generation in muscle [W/m^3]
$q''_{o,comf}$	outside heat loss at comfort cond. [W/m^2]
q''_{skin}	heat flux through skin boundary [W/m^2]
$\dot{Q}$	total heat transfer [W]
$\dot{R}$	latent respiration heat loss [W]
T_a	arterial temperature [℃]
T_c	body core temperature [℃]
T_{ex}	temperature of the expired air [℃]
T_i	skin-fat interface temperature [℃]
T_{s0}	reference temperature [℃], Eq. (20)
T_∞	ambient temperature [℃]
$\bar{T}_s$	average skin temperature [℃]
ΔT_{as}	$T_a - T_{s0}$ [℃]
ΔT_{ac}	$T_a - T_c$ [℃]
ΔT_{ex}	$T_{ex} - T_\infty$ [℃]
u_f	specific internal energy of liquid water [J/kg]
w	specific humidity [kg H_2O/kg dry air]
$\dot{W}_{out}$	work transfer through skin boundary [W]

Greek letters

α_{bm}	pseudo-thermal diffusivity [m^2/s], Eq. (31)
ε	heat efficiency [dimensionless]
ϕ	relative humidity [dimensionless]
η	external mechanical eff. [dimensionless]
θ	excess temperature [℃], Eq. (26)
ρ	density [kg/m^3]
ω	blood perfusion rate [/s]
ω_o	reference blood perfusion rate [/s], Eq. (33)
ω^*	dimensionaless perfusion rate, Eq. (32)

Subscripts

a	dry air
as	asymptotic
b	blood
c	at the body core
$cond$	by conduction
$conv$	by convection
$diff$	by diffusion
f	liquid water
fat	fat
i	at the skin-fat interface
in	into system boundary
m	muscle
out	out of system boundary
$skin$	through skin
sw	by sweating
v	water vapor

external to a human body and related to the successful removal of the heat from the skin to the ambient without considering detailed heat transfer processes inside the body.

Now, questions remain regarding the state inside the body under comfortability conditions. Obviously, the body must dissipate all the heat generated by body activities to maintain a steady comfort state. Heat must flow from the body core to the skin surface then removed by heat transfer mechanisms included in Fanger's model. On the other hand, Fanger's comfortability conditions merely require that the mean skin temperature and sweat evaporation rate be at specific values (without considering heat transfer processes inside the body). If we turn our attention to the inside of the body, two main mechanisms facilitate heat removal from the core to skin surface: heat conduction through body tissues and blood perfusion. Since the thermal properties such as thermal conductivity are almost fixed, conduction alone is not flexible enough to meet the Fanger's comfortability conditions with changing activity level (or heat generation). It is the blood perfusion that provides the required flexibility. Blood perfusion relocates thermal energy in such a way that proper temperature gradient is established to render generated heat successfully conducted away without causing overheating inside the tissue. If conduction and blood perfusion successfully cooperate to achieve a comfortable state, the body can stay in a comfortability zone. Otherwise, the body will end up in a state where it feels uncomfortable. The degree of discomfort is usually indicated by thermal sensation scale (ASHRAE, 2009).

If we know the temperature distribution inside the body a priori, we can delineate the contributions from the two mechanisms of conduction and blood perfusion. However, experiments to measure the temperature distribution and blood perfusion inside a human body is extremely difficult, and there is no such data available at the moment. Installing temperature sensors inside a living body and logging the data is a difficult challenge. The human body must stay in a steady state for an elongated period of time to obtain a valid steady-state data. One possible approach is to find the temperature distribution and blood perfusion intensity by analytically solving an equation that governs the heat transfer processes. We will solve the Pennes bioheat equation (Pennes, 1948) with boundary conditions imposed by Fanger's comfortability conditions to find the temperature distribution and blood perfusion intensity for a body at the steady comfortable condition.

Heat transfer inside the human body is the main topic of this study. Review papers are available for the general topics of bioheat transfer and human comfort. Bhowmik et al. (2013) summarized recent attempts by numerous researchers to model the complex thermal behavior of the human body. They compared the strength and limitations of numerous models such as blood perfusion, countercurrent, thermal phase-lag, porous-media, perturbation, and radiation; and provided various contextual issues associated with them. Recently this journal published a special issue (Shrivastava et al., 2016) on modeling the bioheat transfer processes and thermoregulatory responses. It presented numerous papers on various topics of the computational modeling of thermoregulation. The topics included novel analytical approaches for modeling the bioheat transfer process, computational approaches for solving bioheat transfer models, responses of human subjects to thermal stress, thermoregulation in premature infants, the prediction of the effects of ambient temperature on the heat exchange of the human eye, and the modeling of body heat transfer as it relates to forensic science.

Generally, bioheat transfer and human comfort change with time, and are subject to the nonuniform body conditions and environment.

The recent trend of research demonstrates this (Jović et al., 2016). Khiavi et al. (2018) studied the thermal perception of the human body under non-uniform environments. They included the thermal responses of cutaneous thermoreceptors in different body parts in a time-dependent manner. Zhou et al. (2017) predicted skin temperature and thermal comfort in two-way transient environments. They employed the predicted mean vote (PMV) model, the Fiala model and their Chinese model as thermal sensation models; and compared thermal sensations under transient environmental conditions. Wang et al. (2015) investigated the physiological and psychological human thermal responses in different heating environments of floor heating and radiant heating.

Zolfaghari and Maerefat (2010) proposed a new simplified thermoregulatory bioheat model to describe heat transfer in skin tissue. The time-dependent temperature of the skin tissue was obtained by solving the bioheat equations, taking thermoregulatory mechanisms into account. Salloum et al. (2007) proposed a transient bioheat model of the human body and integrated it with clothing models. A multi-segmented model was developed for the prediction of the nude human thermal and regulatory responses within body segments and the environment. The predictions from the nude and clothed body models were compared with published experimental data at a variety of ambient conditions and activity. Frank et al. (1999) investigated the relative contribution of core and cutaneous temperatures to thermal comfort and autonomic responses in humans, to determine the effects of the core/skin temperature ratio on thermal comfort.

Blood perfusion is an important mechanism for temperature regulation. Acharya et al. (2014) studied the effect of perfusion on the temperature distribution in human bodies in the different thermal environments. The one-dimensional steady version of the bioheat equation was solved using the finite element method, and the skin temperature change with respect to blood perfusion was presented. In a theoretical study, Das and Mishra (2014) demonstrated the equivalence of the Pennes bioheat equation and Wulff continuum model.

A survey of the literature reveals that the development of sophisticated models for more realistic situations, such as nonuniform body temperature and the transient environment, is a recent trend. Many of those studies utilized modern computing power to solve complicated mathematical problems. However, studies focusing exclusively on the thermal comfort condition are rare. Two mechanisms are cooperating to transfer heat generated by human activities (metabolic heat): heat conduction and blood perfusion. According to Fanger (1970), the skin temperature of the body is required to be at a specific value depending on the activity level, to induce thermal comfort in the body. Therefore, the blood perfusion rate and the metabolic rate do not vary independently in the process of meeting all the physical requirements for thermal comfort. In this study, we will investigate how the heat transfer mechanisms cooperate to achieve the neutrality of thermal comfort in response to the changing level of activities and environmental conditions.

The questions we attempt to answer are: what are the mechanisms that enable the human body to dissipate heat to the skin, and how do those mechanisms cooperate to achieve the heat removal task, while meeting all the constraints imposed by the thermal comfort condition (skin temperature) and environmental setup? Many fields are closely related to thermal comfort issues due to their direct impact on human life. Starting from first principles, we will apply an energy balance to the human body as a whole, to obtain a relationship between the activity level and the amount of heat to be removed from the body. Thereafter, we will adopt the classical Pennes bioheat equation (Pennes, 1948) as the governing equation of the heat conduction process. We will include two key parameters of the volumetric heat generation rate and the blood perfusion. The volumetric heat generation represents the immediate local heat conversion by the metabolic process, and blood perfusion represents the relocation of thermal energy by blood flow. A layer of fat will be included in the system to investigate the effect of the added thermal resistance. This study aims to determine the relationships among the key physical variables, under thermal comfort conditions. The temperature and heat flux distributions are also found in the course of the analysis.

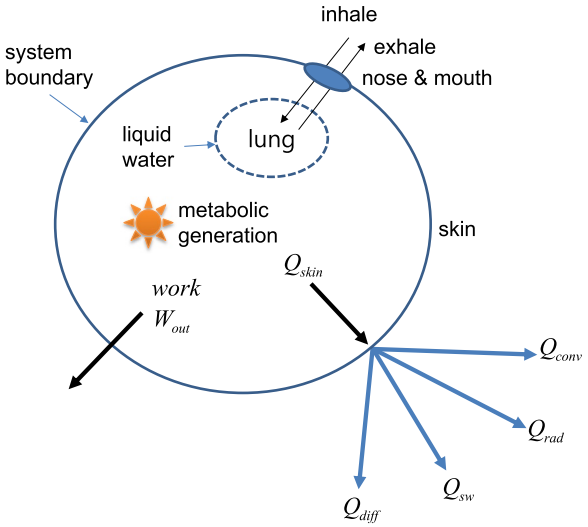

Fig. 1. Schematic diagram of a human body for energy analysis purpose.

2. Model description

2.1. Formulation

2.1.1. Energy balance

Fig. 1 shows a schematic diagram of a human body exchanging energy with the environment. The system boundary consists of the surface of the skin of the body and openings created by the mouth and the nose. The body continuously generates energy by converting the internal energy stored in the food through a chemical process known as digestion. We call this energy conversion metabolic energy generation and denote by the symbol $\dot{M}$. This energy generation depends on activity level and is dissipated to the surroundings through the skin by work (exercise) and heat transfer. Heat is conducted through the system boundary ($\dot{Q}_{skin}$) and transferred away from the skin surface via conduction, convection, radiation, diffusion, and the evaporation of sweat, as indicated in the figure.

We apply the conservation of mass and energy to analyze the mass exchange and energy interaction between the human body and the environment. Two main substances enter and leave the body regularly: air and water. If the production of CO_2 by consuming O_2 during respiration is ignored, the conservation of the mass for dry air is simply

$$\dot{m}_{a,in} = \dot{m}_{a,out} = \dot{m}_a. \tag{1}$$

Water can leave the body through respiration and sweat secretion. Given that transport of water by respiration occurs through the system port (nose and mouse), whereas transport by sweating occurs on the system boundary (skin), separate accounting is convenient. A significant amount of water evaporates from the lung surface during the respiration process. The amount of liquid water supplied to the lung surface is the difference between the moist contents in the exhaling and inhaling air.

$$\dot{m}_f = \dot{m}_{v,out} - \dot{m}_{v,in}. \tag{2}$$

The energy balance (first law of thermodynamics) for a system is expressed as (Moran and Shapiro, 2014):

$$\frac{dE_{sys}}{dt} = \dot{E}_{in} - \dot{E}_{out}. \tag{3}$$

where E_{sys} is the total energy of the system, $\dot{E}_{in}$ and $\dot{E}_{out}$ are the total

energy entering and the total energy leaving the system through the system boundary, respectively. For simple compressible systems where the effects of electricity, magnetism, and surface tension can be ignored, the total energy is the sum of the internal, kinetic, and potential energies (Cengel, 2014). Dealing with the comfort conditions of the human body, we will assume that the system is stationary and the changes in the kinetic and potential energies are negligible. The change of the total energy is then merely the change of the internal energy. If the body changes elevation by activities such as mountain climbing, the change of potential energy can be considered in the form of work. For the analysis, it is convenient to divide the internal energy further, into chemical energy and thermal energy. As mentioned earlier, the rate of change of the chemical energy of food is commonly referred to as the metabolic rate ($\dot{M}$). The portion of energy accounted as the thermal energy of the body is mainly a function of the body temperature. We assume a quasi-steady state where the state of the human body does not change (thermally comfortable). The left-hand side of Eq. (3) is still not zero under this quasi-steady condition, because there are portions of the system that change with time. The following two effects are considered: food is continuously consumed by the digestion process at a rate of $\dot{M}$, and the mass of liquid water is reduced by evaporation at the lung surface during the respiration process at a rate of $\dot{m}_f$. We have the following expression for the change of the total energy of the system:

$$\frac{dE_{sys}}{dt} = -\dot{M} - \dot{m}_f u_f. \tag{4}$$

The minus sign is necessary because the chemical energy of food and internal energy of water is decreased through the digestion and respiration processes.

There are three mechanisms for energy transfer denoted by $\dot{E}_{in}$ and $\dot{E}_{out}$: heat, work, and mass flow. For the system in Fig. 1, all three forms are present. The system can transfer work as the human body performs various forms of physical activities. Heat transfer can occur due to the temperature difference between the system and surroundings. Breathing can bring the air into the system (inhale) and exhaust to the system (exhale). The energy transfer can be expressed as

$$\dot{E}_{in} - \dot{E}_{out} = \sum_{air,H_2O} \dot{m}_{in} h_{in} - \sum_{air,H_2O} \dot{m}_{out} h_{out} - \dot{Q}_{skin} - \dot{W}_{out}. \tag{5}$$

The subscripts *in* and *out* represent the component that enters *into* the system and *out of* the system, respectively. Both heat and work are assumed to leave the body (as indicated by the minus signs). Air is assumed to be an ideal gas mixture of dry air and water vapor, and their kinetic and potential energies are ignored because their magnitudes relative to the change of enthalpy values are negligible (Cengel, 2014). The terms representing energy transfer by mass flow in Eq. (5) can be specified as

$$\begin{aligned}\sum_{air,H_2O} \dot{m}_{out} h_{out} - \sum_{air,H_2O} \dot{m}_{in} h_{in} &= (\dot{m}_a h_a + \dot{m}_v h_v)_{out} \\ &\quad - (\dot{m}_a h_a + \dot{m}_v h_v)_{in} = \dot{m}_a (h_{a,out} - h_{a,in}) \\ &\quad + \dot{m}_a [w_{out} h_{v,out} - w_{in} h_{v,in}].\end{aligned} \tag{6}$$

where w is specific humidity defined as $w = \dot{m}_v / \dot{m}_a$. Traditionally, energy transfer due to sensible energy and latent energy is separately accounted for, and each contribution is called the dry respiration heat loss ($\dot{L}$) and the latent respiration heat loss ($\dot{R}$). A concept of external mechanical efficiency is conveniently used to separate the portion of metabolic energy consumed by work (Fanger, 1970).

$$\eta = \frac{\dot{W}_{out}}{\dot{M}}. \tag{7}$$

The heat efficiency is defined as

$$\varepsilon = \frac{\dot{Q}}{\dot{M}} = \frac{\dot{M} - \dot{W}_{out}}{\dot{M}} = 1 - \eta. \tag{8}$$

Substituting Eqs. (4), (5), (6), (7), and (8) into Eq. (3), we can obtain an expression for heat transfer to the skin, as follows:

$$\begin{aligned}\dot{Q}_{skin} = \dot{M} \underbrace{(1-\eta)}_{\varepsilon} - \underbrace{\dot{m}_a (h_{a,out} - h_{a,in})}_{\dot{L}} \\ - \underbrace{[\dot{m}_a (w_{out} h_{v,out} - w_{in} h_{v,in}) - \dot{m}_f u_f]}_{\dot{R}}.\end{aligned} \tag{9}$$

Dividing this equation by the total skin area, known as DuBois area (A_{Du}), we obtain a heat flux expression at the skin:

$$q''_{skin} = \frac{\dot{Q}_{skin}}{A_{Du}} = \varepsilon \frac{\dot{M}}{A_{Du}} - \frac{\dot{L}}{A_{Du}} - \frac{\dot{R}}{A_{Du}}. \tag{10}$$

2.1.2. Empirical relations

Additional empirical relations are needed to complete the formulation. The objective is to express Eq. (10) in terms of the metabolic rate $\dot{M}$ and parameters directly related to environmental conditions, such as temperature, pressure, and humidity. The air mass flow rate represents the pulmonary ventilation and is known to depend mainly on the metabolic rate. The following linear relationship is widely accepted as a practical approximation for the mean values for different types of work (Fanger, 1970):

$$\dot{m}_a = 0.00516\, \dot{M}. \tag{11}$$

The unit of mass flow rate in the above equation is kg/h, and watt for the metabolic rate. Given that air can be treated as an ideal gas with constant specific heat for our range of interest, the dry respiration heat loss can be expressed as

$$\dot{L} = \dot{m}_a (h_{a,out} - h_{a,in}) = \dot{m}_a c_{pa} (T_{ex} - T_{a,in}), \tag{12}$$

where c_{pa} is the specific heat of dry air at constant pressure, and T_{ex} is the temperature of the expired air. Inserting Eq. (11) into Eq. (12) with the value of $c_{pa} = 1.0035\ \ kJ/kg$, and by conversion to SI units, we obtain the following expression:

$$\dot{L} = C_L \dot{M} (T_{ex} - T_{a,in}), \tag{13}$$

where the constant $C_L = 0.0014\,[/°C]$, and the constant T_{ex} can be assumed to be 34 °C without the loss of accuracy (Fanger, 1970).

The latent respiration heat loss can also be expressed as a function of the metabolic rate and variables representing the environmental conditions. Starting from the definition, we manipulate the expression to obtain an expression that involves air states at inhaling and exhaling.

$$\begin{aligned}\dot{R} &= \dot{m}_a [w_{out} h_{v,out} - w_{in} h_{v,in}] - \dot{m}_f u_f \\ &= \dot{m}_a [w_{in} h_{v,out} - w_{in} h_{v,in} + (w_{out} - w_{in}) h_{v,out}] - \dot{m}_a (w_{out} - w_{in}) u_f \\ &= \dot{m}_a [w_{in} (h_{v,out} - h_{v,in}) + (w_{out} - w_{in})(h_{v,out} - u_f)] \\ &= \dot{m}_a [w_{in} \Delta h_1 + (w_{out} - w_{in})(\Delta h_2 + h_{fg})] \\ &\cong \dot{m}_a (w_{out} - w_{in}) h_{fg},\end{aligned} \tag{14}$$

where the sensible enthalpy difference between the inhaling and exhaling air is defined as $\Delta h_1 = h_{v,out} - h_{v,in}$. The term $w_{in} h_{v,out}$ is added and subtracted, and Eq. (2) is used in the second line of the above derivation. The term $h_{v,out} - u_f$ is manipulated to separate h_{fg} from it. First, the enthalpy of saturated vapor (h_g) is added and subtracted. Then the definition of enthalpy $h_f = u_f + P_v v_f$ is then applied.

$$h_{v,out} - u_f = h_{v,out} - h_g + h_g - h_f + P_v v_f = \Delta h_2 + h_{fg}, \tag{15}$$

where the combined term Δh_2 represents $\Delta h_2 = h_{v,out} - h_g + P_v v_f$. According to the thermodynamic property tables (Cengel, 2014), the magnitudes of the two sensible enthalpy differences (Δh_1, Δh_2) are negligible when compared with the enthalpy of evaporation $h_{fg} = h_g - h_f$. McCutchan and Taylor (1951) developed the following expression for the humidity ratio of the inhaled and exhaled air:

$$w_{out} - w_{in} = 0.029 - 0.00495\, P_v, \tag{16}$$

where P_v is the partial pressure of the water vapor in the air.

Substituting Eqs. (11) and (16) into Eq. (14) with $h_{fg} = 2417.9\ [kJ/kg]$ @35°C, we obtain

$$\dot{R} = C_R \dot{M}\,[\mathrm{W}](P_{ref} - P_v\,[\mathrm{kPa}]). \tag{17}$$

The values of the two constants are $C_R = 0.0172$ [/kPa] and $P_{ref} = 5.86$ [kPa]. Inserting Eqs. (13) and (17) into Eq. (10), we obtain the following working expression for the skin heat flux q''_{skin}:

$$q''_{skin} = \frac{\dot{M}\,[\varepsilon - C_R(P_{ref} - P_v) - C_L(T_{ex} - T_\infty)]}{A_{Du}}. \tag{18}$$

This relationship depends on fixed parameters (C_L, T_{ex}, C_R, P_{ref}) and ambient conditions. The partial pressure of the water vapor can be calculated with the relative humidity, as follows:

$$P_v = \phi P_{sat}(T_\infty), \tag{19}$$

where ϕ is the relative humidity and P_{sat} is the saturation pressure of water at the ambient temperature T_∞.

2.1.3. Fanger comfort criterion

According to the ASHRAE literature (2009), comfort is a condition of mind in which satisfaction with the thermal environment is expressed (Mitchell, 2012). It is a psychological variable rather than a physical variable, and it depends on human perception. One of the best-known criteria for the human perception of thermal comfort is the one proposed by Fanger. Fanger developed a pair of relationships for thermal comfort as a function of activity level ($\dot{M}$), using a regression analysis of experimental data (Fanger, 1970). One relationship is for average skin temperature, as given below.

$$\bar{T}_s = T_{s0} - C_T q''_{skin}. \tag{20}$$

The values of the constants are $T_{s0} = 35.7\ [°C]$ and $C_T = 0.0275\ [°\mathrm{C}\cdot\mathrm{m}^2/W]$. The other relationship is for average sweat secretion:

$$\frac{\bar{E}_s}{A_{Du}} = C_E(q''_{skin} - q''_{s0}), \tag{21}$$

where the values of the constants are $C_E = 0.42$ and $q''_{s0} = 58.15\ [\mathrm{W/m^2}]$. It is important to realize that the two relationships are concerned with the conditions on the body itself, regardless of external conditions. According to Eq. (20), there is a tendency for human bodies to maintain the skin temperature at lower temperatures when the activity level is high, to induce thermal comfort. It is the role of air conditioning to match the outside conditions (including clothing) with the comfort conditions by adjusting surrounding conditions such as ambient temperature and humidity.

For a body under comfort conditions, Eqs. (20) and (21) provide significant computational convenience for calculating outside heat transfer from the skin to the ambient. First, the heat loss from the skin to the environment (the outside heat loss at comfort condition, $q''_{o,comf}$) can be easily calculated. The heat transfer nodes associated with $q''_{o,comf}$ include the skin, the clothing, and the ambient. With a known temperature difference of endpoints ($\Delta T = \bar{T}_s - T_\infty$) and the total thermal resistance (R_{tot}), the heat loss $q''_{o,comf} = \Delta T / R_{tot}$. The total thermal resistance includes the effects of conduction and radiation through the clothing, convection, and radiation at the exposed surfaces. Second, a quantity known as the thermal load can be estimated by finding the difference between the heat flux due to the removal actual internal heat generation (q''_{skin}) and the total heat loss under the comfort condition [$q''_{o,comf}$ plus the sweat secretion specified by Eq. (21)]. The value of the thermal load is zero when a body is under the comfort conditions, and the degree of discomfort is greater the larger the thermal load value is. Correlations based on the thermal load are widely used in the traditional assessment of thermal environments (Fanger, 1970, ANSI/ASHRAE Standard 2004, ISO, 2005).

In this study, we will analyze the conduction heat transfer inside the body and the Fanger comfort conditions serve different purpose. We only focus on the conditions of thermal comfort, and off-comfort conditions are not considered. The relationship for skin temperature, Eq. (20), will be used as a boundary condition of a differential equation governing the conduction inside the body, in the subsequent analysis. The condition for sweat secretion, Eq. (21), is already included in the overall energy balance but will not be directly used in the heat transfer analysis. The reason for this is that the comfort condition considers only the body itself (within the skin boundary), without considering outside heat transfer from the skin to ambient. Ensuring that the skin temperature is at the comfort condition by suitably adjusting environmental conditions such as clothing and air temperature (or making the thermal load near zero) is a separate problem. Failing to do so results in a certain degree of discomfort, and this scenario is beyond the scope of this study.

2.1.4. Pennes bio-heat equation

Pennes (1948) introduced a modification to the heat conduction equation to account for blood perfusion effects in living tissues. It is called *the bioheat equation.* Significant efforts have been devoted to improving the contents of the Pennes equation, as summarized in the literature survey section of the introduction. As mentioned by Arkin et al. (1994), the modeling of heat transfer in living tissues is a difficult task, and some simplified assumptions are needed. Some investigators (Wulff, 1974; Klinger, 1974) have argued that the Pennes interpretation of the vascular contribution to heat transfer in perfused tissues fails to account for the actual thermal equilibration process between the flowing blood and the surrounding tissue. Furthermore, new models (Mitchell and Myers, 1968; Chen and Holmes, 1980; Weinhaum and Jiji, 1985) were proposed, presumably based on a more realistic anatomy of the perfused tissue. However, the new models still lack sound experimental grounding, and considering their inherent complexity; the bioheat equation is still useful for the study of the basic heat transfer problems involving living tissues.

Fig. 2 shows the schematic diagram for the heat transfer analysis in a combined layer of muscle and fat of the human body. As mentioned earlier, heat transfer outside of the skin is beyond the scope of this study, and physical quantities for the external region shown in the figure are for information purposes only.

To focus on the role of the key mechanisms of the metabolic rate and blood perfusion under thermal comfort conditions, we will adopt the following assumptions:

1. The state conditions are quasi-steady under Fanger thermal comfort conditions.
2. There is one-dimensional heat transfer through combined slab layers of muscle and fat.

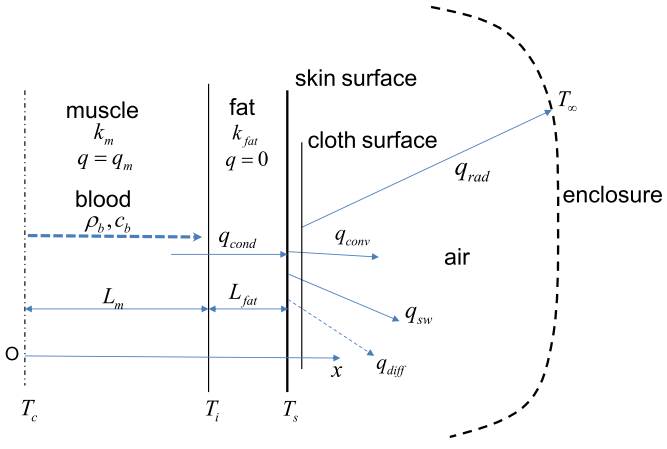

Fig. 2. Schematic for one-dimensional heat transfer.

3. The arterial temperature, blood properties, and thermal conductivities are constant.
4. The values of metabolic heat generation rate and perfusion rate are uniform over space.
5. There is no heat generation in the fat layer.

Pennes proposed the expression for heat transfer due to blood perfusion by assuming that blood flowing into small capillaries enters at an arterial temperature and exits at the local tissue temperature. The heat transfer from the blood to the tissue can be expressed as

$$\dot{q}_p = \omega\rho_b c_b(T_a - T), \tag{22}$$

where ω is the blood perfusion rate, T_a is the arterial temperature, and ρ_b, c_b are the density and the specific heat of blood, respectively. For a transient problem, the one-dimensional Pennes bioheat equation is given as:

$$\rho_m c_m \frac{\partial T}{\partial t} = k_m \frac{\partial^2 T}{\partial x^2} + \dot{q}_p + \dot{q}_m. \tag{23}$$

where $T(x, t)$ represents the local temperature distribution, ρ_m, c_m, k_m are the muscle density, specific heat and thermal conductivity, respectively. $\dot{q}_m$ is the volumetric metabolic rate in the muscle. Note that the *volumetric* metabolic heat generation $\dot{q}_m$ $[W/m^3]$ should be distinguished from the total metabolic heat generation rate $\dot{M}$[W], which represents the total heat generation in the entire body.

Our study focuses only on equilibrium conditions satisfying the comfortability requirement in Fanger's sense and transient effects will be ignored. The Fanger model is the simplest one and the physiological parameters and thermoregulatory mechanisms of the human body have not been considered. The body thermal signals cannot be incorporated into the model as a result of dropping the transient term. Modifying Eq. (23) by dropping the transient term and including the blood perfusion term given in Eq. (22), we can obtain the following steady bioheat equation (Incropera et al., 2012):

$$\frac{d^2T}{dx^2} + \frac{\dot{q}_m + \omega\rho_b c_b(T_a - T)}{k_m} = 0, \tag{24}$$

The bioheat equation is a second order differential equation, and two boundary conditions are required. The temperature at the origin is the body core temperature T_c, which is known to be 36.5 °C. The link between the Pennes equation and the Fanger model is established through the boundary condition for the governing equation. The average skin temperature given by Eq. (20) serves as a boundary condition for Eq. (24) as explained in Section 2.2.2. As there exists an additional node of a fat layer, the skin temperature specified by Fanger's comfort criteria is indirectly applied. A Dirichlet boundary condition is imposed at the muscle-fat interface with the value of T_i, which is unknown for now. The mathematical expressions for the two boundary conditions are:

$$\begin{aligned} T(0) &= T_c \\ T(L_m) &= T_i \end{aligned}. \tag{25}$$

2.2. Analysis

2.2.1. Formal solution

We will follow the same procedure as described in the textbook (Incropera et al., 2012) to determine the solution of the bioheat equation. First, we define an excess temperature as

$$\theta = T - T_a - \frac{\dot{q}_m}{\omega\rho_b c_b}. \tag{26}$$

Based on the assumption that T_a, $\dot{q}_m$, ω and the properties are constant, the bioheat Eq. (24) can be transformed to

$$\frac{d^2\theta}{dx^2} - m^2\theta = 0, \tag{27}$$

where $m = \sqrt{\omega\rho_b c_b/k_m}$. The solution to this equation with boundary conditions subject to Eq. (25) is

$$\theta = \frac{\theta_i \sinh mx + \theta_c \sinh m(L_m - x)}{\sinh mL_m}, \tag{28}$$

where the transformed boundary excess temperatures are

$$\theta_c = T_c - T_a - \frac{\dot{q}_m}{\omega\rho_b c_b}, \tag{29}$$

$$\theta_i = T_i - T_a - \frac{\dot{q}_m}{\omega\rho_b c_b}. \tag{30}$$

It is convenient to define a pseudo-thermal diffusivity as

$$\alpha_{bm} = \frac{k_m}{\rho_b c_b}. \tag{31}$$

This is not a true thermal diffusivity because the properties are partly from the muscle and partly from the blood. We can give the following physical meaning to the dimensionless term mL_m:

$$mL_m = \sqrt{\frac{\omega\rho_b c_b L_m^2}{k_m}} = \sqrt{\frac{\omega}{\omega_o}} = \sqrt{\omega^*} \tag{32}$$

with the reference blood perfusion defined as

$$\omega_o = \frac{\alpha_{bm}}{L_m^2} \quad \left[\frac{\mathrm{m}^2/s}{\mathrm{m}^2} = \frac{1}{\mathrm{s}}\right]. \tag{33}$$

The dimension of ω_o is 1/s, as specified within the brackets of the above equation.

2.2.2. Application of Fanger comfort condition and system energy balance

The Fanger comfort condition, Eq. (20), specifies the skin temperature as a function of the total metabolic rate at the outer side of the fat layer. The boundary condition for the bioheat equation, Eq. (25), is specified at the muscle-fat interface, which is located within the skin. An additional heat transfer node is required to account for the fat layer. The continuity of the conduction heat flux across the muscle-fat interface and through the fat layer requires

$$q''_{skin} = k_{fat}\frac{T_i - T_s}{L_{fat}}. \tag{34}$$

Inserting expressions for q''_{skin}, Eq. (18), and the skin temperature proposed by Fanger, Eq. (20), into the above equation and solving for T_i, we can determine the interface temperature:

$$T_i = T_{s0} + \frac{\dot{M}}{A_{Du}k_{fat}}[(C_R\Delta P_v - C_L\Delta T_{ex} + \varepsilon)L_{fat} - k_{fat}C_T\varepsilon], \tag{35}$$

where $\Delta T_{ex} = T_{ex} - T_\infty$ and $\Delta P_v = P_v - P_{ref}$, respectively.

The continuity of the conduction heat flux across the muscle-fat interface requires that

$$q''_{skin} = -k_m\frac{dT}{dx}\bigg|_{x=L_m} = -k_m\frac{d\theta}{dx}\bigg|_{x=L_m} = -k_m m\frac{\theta_i\cosh mL_m - \theta_c}{\sinh mL_m}. \tag{36}$$

Inserting expressions for q''_{skin} [Eq. (10)], θ_c [(Eq. (29)], θ_i[Eq. (30)], and the expression for T_i [Eq. (35)] into the above equation, the following relationship between the volumetric metabolic rate ($\dot{q}_m$) and blood perfusion (ω) is obtained:

$$\dot{q}_m^{\,i} = \frac{\rho_b c_b \omega \coth(mL_m/2)}{A_{Du} k_{fat} k_m m} \begin{bmatrix} -k_m m\{\dot{M}[\varepsilon(C_T k_{fat} - L_{fat}) - L_{fat}(C_R \Delta P_v - C_L \Delta T_{ex})] \\ \quad - A_{Du} \Delta T_{as}\} \coth mL_m \\ +k_{fat}\{\dot{M}(C_R \Delta P_v - C_L \Delta T_{ex} + \varepsilon) + A_{Du} k_m m \Delta T_{ac} \operatorname{csch} mL_m\} \end{bmatrix}, \tag{37}$$

where $\Delta T_{as} = T_a - T_{s0}$, $\Delta T_{ac} = T_a - T_c$. Remembering that $m = \sqrt{\omega \rho_b c_b / k_m}$, the right side of the above equation is a function of ω, for given values of $\dot{M}$ and parameters describing operating conditions. The superscript i in $\dot{q}_m^{\,i}$ indicates that the value is evaluated at the skin-fat *interface*. Note that the following mathematical identity is used in deriving the above equation.

$$\frac{\sinh x}{\cosh x - 1} = \coth \frac{x}{2}. \tag{38}$$

The relationship represented by Eq. (37) is plotted in Fig. 3 as a function of ω, for a set of different values of $\dot{M}$. The solid lines represent the functional relationships of Eq. (37), whereas the dotted lines represent the asymptotic relations discussed later. We used Mathematica (2011) for the symbolic manipulation of equations and for graphical plots.

The length of the muscle layer is a characteristic length of the human body and evaluated using a formula $L_c = 3V/A$ where V is the volume, and A is the surface area of an object. This formula will yield the radius when applied to a sphere, and half of the side length for a cube. With the values of the volume and the surface area in Table 2, L_c is around 0.1 m for an average human body.

2.2.3. Auxiliary condition at the origin

An additional relationship is required to determine a pair of values, $\dot{q}_m$ and ω, for a given value of $\dot{M}$ and a set of parameters. One possible approach is to directly relate the volumetric metabolic rate $\dot{q}_m$ in muscle to the total metabolic rate $\dot{M}$. Information is required on the part-by-part contribution to the total metabolic rate, to relate the two variables. An alternative method is to impose an adiabatic condition at the origin (near the body core), causing the temperature distribution to have a zero gradient at $x = 0$. Imposing this condition implies that the heat removed from the skin surface is the sum of the heat generated in the muscle layer and transported by blood perfusion. The adiabatic condition can be viewed as a self-supply of heat for the system. In addition to the implication of overall energy balance, our test revealed that the adiabatic condition also helps render well-behaving temperature distribution without overshooting and other irregularities.

To impose the adiabatic condition, we use the derivative of the solution given in Eq. (28) to obtain

$$\left.\frac{dT}{dx}\right|_{x=0} = \left.\frac{d\theta}{dx}\right|_{x=0} = m\frac{\theta_i \cosh 0 - \theta_c \cosh mL_m}{\sinh mL_m} = 0. \tag{39}$$

Inserting expressions for θ_i and θ_c [Eqs. (29), (30)], and then solving for $\dot{q}_m$, we obtain the following relationship:

$$\dot{q}_m = \frac{\rho_b c_b \omega[(T_c - T_a)\cosh mL_m + T_a - T_i]}{\cosh mL_m - 1}. \tag{40}$$

Substituting T_i from Eq. (35), this relationship becomes

$$\dot{q}_m^{\,c} = \frac{\rho_b c_b \omega[A_{Du} k_{fat}(\Delta T_{as} - \Delta T_{ac} \cosh mL_m) + \{\varepsilon C_T k_{fat} - (C_R \Delta P_v - C_L \Delta T_{ex} + \varepsilon) L_{fat}\}\dot{M}]}{A_{Du} k_{fat}(\cosh mL_m - 1)}, \tag{41}$$

where $\Delta T_{ac} = T_a - T_c$. Eqs. (37) and (41) are a pair of relationships that determine the values of $\dot{q}_m$ and ω for a given value of $\dot{M}$ and a set of parameters that specify the environmental conditions. The superscript c in $\dot{q}_m^{\,c}$ indicates that the value is evaluated from the boundary condition at the core of the body where $x = 0$. In Fig. 4, the relationship represented by Eq. (41) is plotted as a function of ω for a set of difference values of $\dot{M}$.

2.2.4. Overall energy balance

If the adiabatic boundary condition is applied at $x = 0$, the sum of the volumetric metabolic heat and the heat transferred through blood perfusion must equal to the heat conducted away from the skin. Per unit skin area, the total heat generated in the system through muscle metabolism and blood perfusion can be calculated as

$$\dot{q}_{total} = \int_0^{L_m} (\dot{q}_m + \dot{q}_p) dx = \int_0^{L_m} [\dot{q}_m + \omega \rho_b c_b (T_a - T)] dx = -\omega \rho_b c_b \int_0^{L_m} \theta dx \tag{42}$$

The adiabatic condition given by Eq. (38) provides the following relationship at $x = 0$:

$$\theta_i = \theta_c \cosh mL_m. \tag{43}$$

Performing the integration with the solution given in Eq. (28), with the definition of θ given in Eq. (26), we obtain

$$\int_0^{L_m} \theta dx = \frac{\theta_i + \theta_c}{m} \frac{\cosh mL_m - 1}{\sinh mL_m}. \tag{44}$$

Inserting Eqs. (43) and (44) into Eq. (42)

$$\dot{q}_{total} = -\omega \rho_b c_b \int_0^{L_m} \theta dx = -\frac{\omega \rho_b c_b \theta_c}{m \sinh mL_m}(\cosh mL_m + 1)(\cosh mL_m - 1). \tag{45}$$

The heat flux at the skin is

$$q''_{skin} = -k_m m \frac{\theta_i \cosh mL_m - \theta_c}{\sinh mL_m} = \frac{-k_m m \theta_c}{\sinh mL_m}(\cosh mL_m + 1)(\cosh mL_m - 1). \tag{46}$$

Given that $m = \sqrt{\omega \rho_b c_b / k_m}$, it can be concluded that $\dot{q}_{total}$ (per unit skin area) $= q''_{skin}$ if the adiabatic condition is imposed. This clearly implies that the sum of the energy gained inside the system by blood perfusion and the volumetric metabolic process in the muscle layer is equal to the heat conducted away from the skin surface, if an adiabatic condition is imposed at the surface of $x = 0$.

2.2.5. Link between Fanger model and Pennes equation

As mentioned earlier in the introduction, Fanger's model deals only with physical quantities associated with the exterior of the body. It is the Pennes equation that provides detailed information about the heat transfer processes inside the body. The linkage between the two models comes through the boundary conditions of the Pennes equation. The skin temperature required by the Fanger model to be in a thermally comfortable state, Eq. (20), serves as the boundary condition specified by Eq. (25) via Eq. (34). The indirect application of the boundary condition is due to the existence of an additional fat layer. The sweat

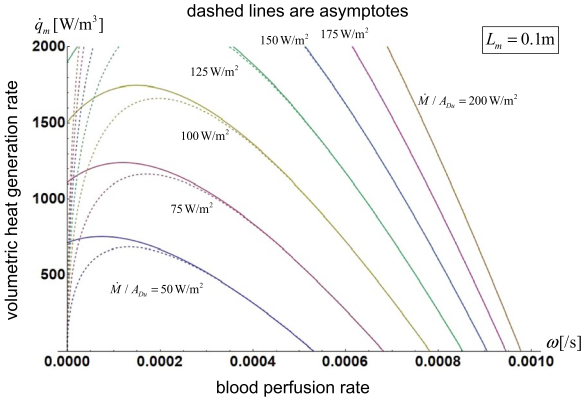

Fig. 3. Relationship between blood perfusion and metabolic heat generation, Eq. (37).

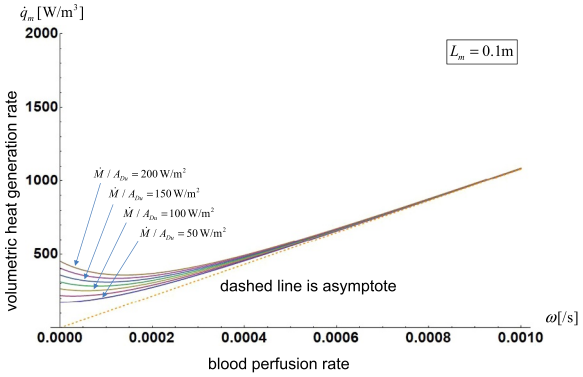

Fig. 4. Relation between blood perfusion and metabolic heat generation, Eq. (41).

secretion condition, Eq. (21), is realized through the boundary condition specified by Eq. (36).

3. Results and discussions

Several coefficients and parameter values are required to evaluate solutions. Tables 1, 2 list the values and the ranges of the values used in our calculations. The values in the tables are selected from existing references (Incropera et al., 2012; Çetingül and Herman, 2010). We calculated the value of the saturation pressure of water $P_{sat}(T)$ using the relationship given in ASHRAE Fundamentals Handbook (2009).

3.1. Relations for blood perfusion and volumetric metabolic generation

For a given value of the total metabolic rate $\dot{M}$, the values of blood perfusion and the volumetric metabolic rate can be obtained by solving Eqs. (37) and (41) for ω and $\dot{q}_m$. The two equations are nonlinear, and no exact solutions are available. Fig. 5 shows the two families of curves for the two equations, and the intersections representing the solutions.

We used Mathematica (2011) to numerically solve the nonlinear equations using the *FindRoot* function of the package. Once the values of ω and $\dot{q}_m$ are determined, the values of θ_c and θ_i can be calculated using Eqs. (29) and (30), and the temperature distribution, are determined using Eq. (28).

3.2. The effect of muscle layer thickness

As mentioned earlier, imposing an adiabatic boundary condition at the center of the muscle layer ($x = 0$) has a significant implication. It forces a self-supply condition of heat, i.e., heat leaving the skin surface must be produced inside the system, either by metabolic heat generation or blood perfusion. The consequence is that a higher heat generation rate is required as the system volume shrinks. Moreover, unlike metabolism, blood perfusion does not generate heat. It relocates thermal energy to a location where the local temperature deviates from the arterial temperature. Heat must be absorbed by the blood somewhere to keep the recycling process steady. We calculated the metabolic heat generation rate as a function of the total metabolic rate $\dot{M}$ by solving Eqs. (37) and (41) for different values of muscle layer thickness, as shown in Fig. 6.

We generated curves, as shown in the figure, by changing the thickness of the muscle layer, from 0.04 m to 0.2 m, in 0.01 m increments. We can observe that $\dot{q}_m$ is not a linear function of $\dot{M}$ because the skin surface temperature drops as $\dot{M}$ increases by the Fanger comfort requirement, Eq. (20). Physically, this helps create a larger temperature gradient at the skin, for higher metabolic heat generation (see Fig. 9). As discussed at the beginning of this section, a higher $\dot{q}_m$ is required as the muscle layer thickness L_m decreases. An interesting observation is that the curve converges to the curve marked as *asymptote*, as L_m increases. The asymptotic behavior is discussed in a separate section below. The asymptotic values indicate the lower limit for $\dot{q}_m$.

Fig. 7 shows the results for blood perfusion, ω, for the same set of muscle layer thickness values shown in Fig. 6.

Again, the effect of the muscle layer thickness is significant for the case of blood perfusion ω, and a similar trend of functional dependence on $\dot{M}$ is observed. The reason for the similarity is explained along with the discussion of the asymptotic behavior below. The asymptotic values for blood perfusion indicate the upper limit, as shown in the figure.

3.3. The effect of fat layer thickness

In Fig. 8, a group of curves is generated by changing the thickness of the fat layer, from 0.001 m to 0.005 m, in 0.001 m increments, with a fixed value of $L_m = 0.1$ m.

The fat layer adds heat transfer resistance to the heat conduction path, and the temperature gradient is reduced. Less heat removal by conduction requires a higher blood perfusion rate for the same amount of heat to be removed. The effect of the fat layer is substantial, and the rate of increase of blood perfusion increases as the fat thickness increases. The range of the value of fat thickness is selected based on reported values by Çetingül and Herman (2010).

3.4. Temperature distribution

The comfort condition proposed by Fanger, Eq. (20), is imposed as a boundary condition at the skin surface. Fig. 10 shows the effect of activity level on temperature distribution for cases without a fat layer. In accordance with Eq. (20), higher activity level lowers the skin temperature to help create a higher temperature gradient at the skin surface. Higher values of gradient are required for the muscle to pass the larger amount of heat generated by the elevated metabolism.

Fig. 10 shows the temperature distribution for a case of the metabolic rate of 150 W/m^2. Nine curves are shown for different muscle layer thicknesses, from 0.04 m to 0.2 m, in 0.02 m increments. A boundary layer type temperature distribution (temperature change occurs only in a narrow region near the skin) is observed. The shapes of the temperature distribution at the tip (near the skin surface) are similar, regardless of the muscle thickness. Moreover, the temperature remains flat near the core of the body, as required by the adiabatic condition. When the local temperature is below the arterial temperature (T_a), heat is transferred from the blood to muscle, and vice versa. This means that blood perfusion absorbs the heat generated by metabolism near the core of the body and discharges into the region near the skin surface, where the temperature drops below the arterial temperature.

3.5. Asymptotic behavior of solutions

All the previous results reveal asymptotic trends. The asymptotic behavior stems from the hyperbolic functions in Eqs. (37) and (41), and it is the value of $mL_m = \sqrt{\omega^*}$ [dimensionless blood perfusion, Eq. (32)] that controls the convergence. In Eq. (37), both $\coth mL_m$ and $\coth(mL_m/2)$ rapidly converge to unity, whereas $\mathrm{csch} mL_m$ converges to zero as mL_m increases. From Eq. (37), the asymptote is

Table 1
List of coefficient values.

parameter	value	unit	Remark
C_R	0.0173	/kPa	Eq. (17)
P_{ref}	5.867	kPa	Eq. (17)
C_L	0.0014	/°C	Eq. (13)
T_{ex}	34	°C	Eq. (13)
T_{s0}	35.7	°C	Eq. (20)
C_T	0.0275	°C·m^2/W	Eq. (20)

Table 2
List of parameter values.

parameter	value	unit	Remark
ρ_b	1000	kg/m^3	blood density
c_b	3600	J/kg-K	blood specific heat
k_{ms}	0.5	W/m-K	muscle thermal conductivity
k_{fat}	0.3	W/m-K	fat thermal conductivity
L_{fat}	0.001–0.005	m	fat thickness
T_c	36.5	°C	body core temperature
T_a	36.2	°C	arterial temperature
A_{Du}	1.77	m^2	DuBois area
V	0.071	m^3	body volume (70 kg person)
ϕ	50	dimensionless	relative humidity
T_∞	15	°C	ambient temperature
ε	1	dimensionless	heat efficiency, Eq. (8)
L_m	0.004–0.2	m	muscle layer thickness

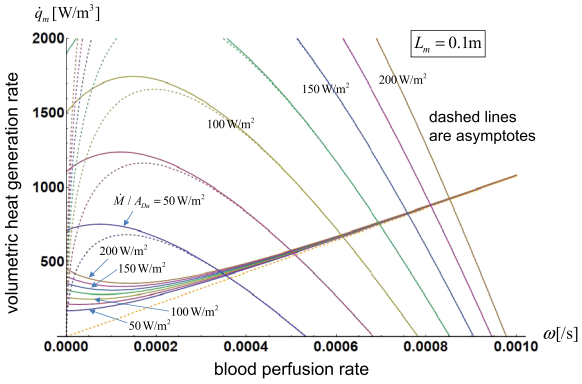

Fig. 5. Graphic representation of solutions of Eq. (36) and Eq. (40).

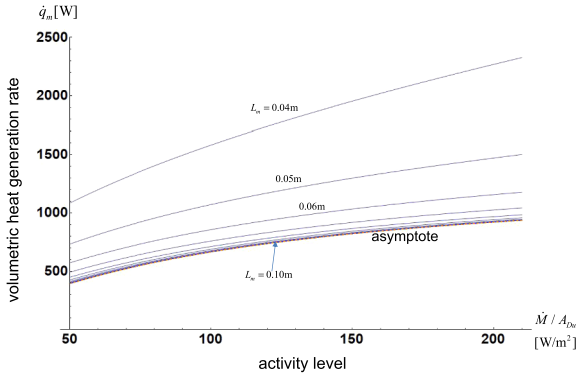

Fig. 6. Effect of muscle layer thickness on metabolic heat generation in muscle.

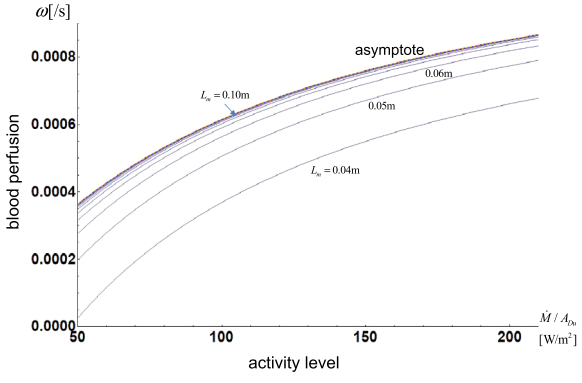

Fig. 7. Effect of muscle layer thickness on blood perfusion.

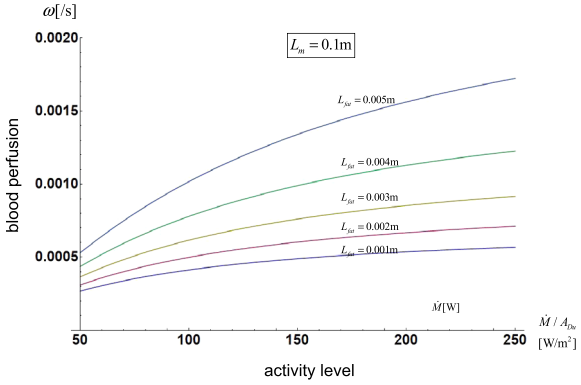

Fig. 8. Effect of fat layer thickness on metabolic heat generation.

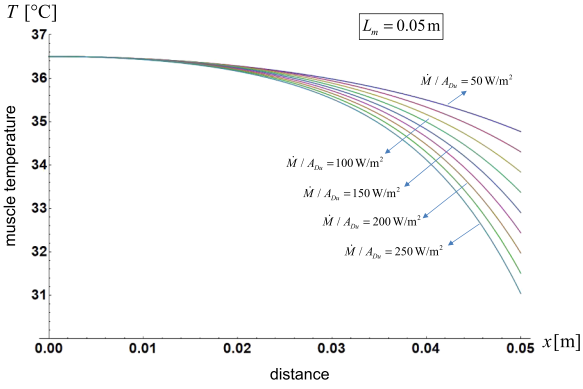

Fig. 9. Effect of activity level on temperature profile.

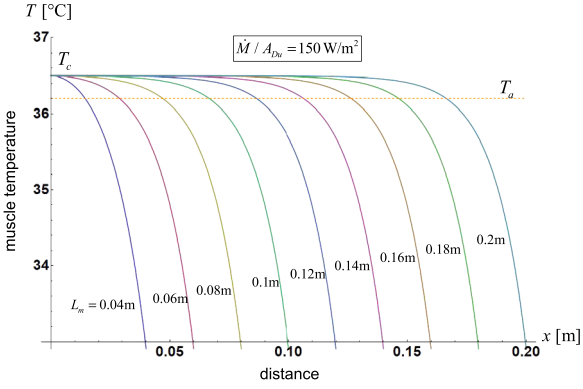

Fig. 10. Effect of muscle layer thickness on temperature profile.

$$\lim_{mL_m \to \infty} \dot{q}_m^i = \frac{\rho_b c_b \omega}{A_{Du} k_m m}[\dot{M}(C_R \Delta P_v - C_L \Delta T_{ex} + \varepsilon)] - \frac{\rho_b c_b \omega}{A_{Du} k_{fat}}[\dot{M}\{\varepsilon(C_T k_{fat} - L_{fat}) - L_{fat}(C_R \Delta P_v - C_L \Delta T_{ex})\} - A_{Du} \Delta T_{as}] = A\omega + B\sqrt{\omega} \tag{47}$$

where the parameter groups A and B are defined as

$$A = -\frac{\rho_b c_b}{A_{Du} k_{fat}}[\dot{M}\{\varepsilon(C_T k_{fat} - L_{fat}) - L_{fat}(C_R \Delta P_v - C_L \Delta T_{ex})\} - A_{Du} \Delta T_{as}]$$

$$B = \frac{1}{A_{Du}} \sqrt{\frac{\rho_b c_b}{k_m}} [\dot{M}(C_R \Delta P_v - C_L \Delta T_{ex} + \varepsilon)] \tag{48}$$

In Eq. (41), it is $\cosh mL_m$ that controls the asymptotic behavior. Note that the combined term $\cosh mL_m/(\cosh mL_m - 1)$ rapidly converges to unity as mL_m increases.

$$\lim_{mL_m\to\infty} \dot{q}_m^c = -\rho_b c_b \omega \Delta T_{ac} = -\frac{L_m^2}{\alpha_{bm}}\frac{k_m}{L_m^2}\omega\Delta T_{ac} = C\omega$$
$$= -\frac{k_m}{L_m^2}\Delta T_{ac}\omega^*; \quad \omega^* = \omega/\omega_o; \quad \omega_o = \frac{\alpha_{bm}}{L_m^2} \tag{49}$$

where the parameter group C is defined as

$$C = -\frac{L_m^2}{\alpha_{bm}}\frac{k_m}{L_m^2}\Delta T_{ac} \tag{50}$$

In many cases, the value of ω_0 is in the order of 10^{-6}, whereas ω is in the order of 10^{-4}. Hence, the values of ω^* are in the range of 10–100, which produces favorable conditions for using the asymptotic expressions of Eqs. (47) and (49) instead of Eqs. (37) and (41). A plot for the case where an asymptotic approach produces a poor result is provided in Fig. 11 to contrast with the case where the asymptotic approach is favorable (i.e., the case shown in Fig. 5). Unlike in Fig. 5, the solutions obtained from the original equations [circles representing the intersections of Eqs. (37) and (41)] and those obtained from the asymptotes [squares representing the intersections of Eqs. (47) and (49)] are far separated.

Asymptotic behavior is also dominant in the temperature distribution. Fig. 12 shows the temperature distribution at the right tips of the calculation domain. The curves are produced by clipping the right side of each curve in Fig. 10 and then combining the clipped curves. The figure reveals that the temperature distribution converges as L_m increases. The symbol x_{clip} means the distance from the origin to the left edge of the clipped tips.

3.6. Closed form of solutions from asymptotic analysis

Owing to the asymptotic characteristics of the problem at hand, it is possible to obtain explicit expressions for the values of blood perfusion and the volumetric heat generation rate. Requiring $\dot{q}_m^c = \dot{q}_m^i$ for the expressions in Eqs. (47) and (49), an expression for ω can be obtained, as follows:

$$A\omega + B\sqrt{\omega} = C\omega$$
$$\omega = \left(\frac{B}{C-A}\right)^2$$
$$\omega_{as} = \frac{[(C_R\Delta P_v - C_L\Delta T_{ex} + \varepsilon)k_{fat}\dot{M}]^2}{\rho_b c_b k_m [A_{Du}(\Delta T_{as} - \Delta T_{ac})k_{fat} + \{C_T\varepsilon k_{fat} - (C_R\Delta P_v - C_L\Delta T_{ex} + \varepsilon)L_{fat}\}\dot{M}]^2} \tag{51}$$

$$\dot{q}_{m,as} = C\omega_{as} = -\rho_b c_b \Delta T_{ac}\omega_{as} \tag{52}$$

The subscript $_{as}$, in the above equations, stands for *asymptotic*. The relationships are plotted in Figs. 6 and 7 using dashed lines. It is worth noting that Eq. (52) represents the equilibrium condition of $\dot{q}_m = \dot{q}_p$. At equilibrium, the heat generated by the volumetric metabolic process is locally absorbed by blood perfusion. Adding the region of muscle at the same temperature as the core temperature (equilibrium region) to the existing layer of muscle does not affect the overall energy balance. This fact is the underlying cause of the asymptotic behavior beyond a certain muscle layer thickness. The overall energy balance was obtained by forcing the adiabatic condition at the core of the body. Based on this observation, it can be concluded that it is sufficient to consider only the muscle region where temperature changes (the boundary layer), and the extent of the region beyond it is irrelevant to the overall energy balance. Therefore, the explicit relationship presented in Eqs. (51) and (52) may be sufficient for cases where the only consideration is the average behavior of a human body as a lumped system.

The two expressions yield the values of blood perfusion and the volumetric metabolic rate under Fanger comfort conditions, for a given activity level ($\dot{M}$) and a set of environmental conditions. It should be noted that neither Eq. (51) nor (52) contains L_m. However, a specific value of L_m is still required to determine the temperature distribution using the solution given by Eq. (28), even if the asymptotic values obtained from Eqs. (51) and (52) are used. A sufficiently large value of the thickness is recommended (for example L_m = 0.2m), and the temperature distribution can then be evaluated using Eqs. (28)–(30) with the asymptotic values of ω, and $\dot{q}_m$ calculated using Eqs. (51) and (52). The profiles from the far-right hand portion can then be used as the temperature profile.

The asymptotic convergence of the temperature profiles shown in Fig. 12 can be explained as follows. The value of m in Eq. (28) determines the shape of the temperature profile. By definition, $m = \sqrt{\omega\rho_b c_b/k_m}$, and m depends on ω and the properties of muscle and blood. The value of m converges to a fixed value as ω converges to an asymptotic value, as L_m increases. The contribution from the first term in Eq. (28) near the edge ($x \to L_m$) decreases as L_m increases. Therefore, the temperature distribution near the right edge converges to a shape specified by the second term of Eq. (28), i.e.

$$\lim_{x\to L_m}\theta = \frac{\theta_i \sinh mx + \theta_c \sinh m(L_m - x)}{\sinh mL_m} \to \frac{\theta_i \sinh mx}{\sinh mL_m} \to \theta_i\frac{e^{mx}}{e^{mL_m}}$$
$$= \theta_i e^{m(x-L_m)} \tag{53}$$

We can see that the asymptotic temperature distribution in the above equation depends on a single independent variable (the distance from the edge in the negative direction, x-L_m) and two parameters (θ_i and m). The explicit expression for the asymptotic temperature distribution can be obtained from the definition of θ, Eq. (26):

$$T(\tilde{x}) = T_a + \frac{\dot{q}_m}{\omega\rho_b c_b} + \left(T_i - T_a - \frac{\dot{q}_m}{\omega\rho_b c_b}\right)e^{-m\tilde{x}} = T_c + (T_i - T_c)e^{-m\tilde{x}} \tag{54}$$

where $\tilde{x} = L_m - x$, the distance from the edge in the negative direction. When the asymptotic expressions for $\dot{q}_m$ and ω obtained from Eqs. (51) and (52) are substituted into the first line of Eq. (54), the expression in the second line is obtained. The parameter value of m is evaluated using $\sqrt{\omega\rho_b c_b/k_m}$ by definition, and the muscle-fat interface temperature T_i is specified by Eq. (35). The thick dotted line in Fig. 12 represents the asymptotic temperature obtained using Eq. (54). The temperature distribution given by Eq. (54) satisfies the governing equation and the boundary condition at the skin/fat interface, and asymptotically satisfies the adiabatic boundary condition at $x = 0$.

Our numerical test revealed that the results are particularly sensitive to the parameter value of ΔT_{ac}. This is not surprising because ΔT_{ac} controls the slope of the curves in Fig. 4 as seen clearly in the asymptotic relation of Eq. (49), and eventually affects the loci of the solutions (see Fig. 5). For body core temperature (T_c) of 36.5 °C, we chose the arterial temperature value of 36.2 °C, which yields $\Delta T_{ac} = T_c - T_a = 0.3°C$. With this value of ΔT_{ac}, our calculation results fall within the ranges of reported values, for example, Çetingül and Herman (2010) and Icropera et al. (2012).

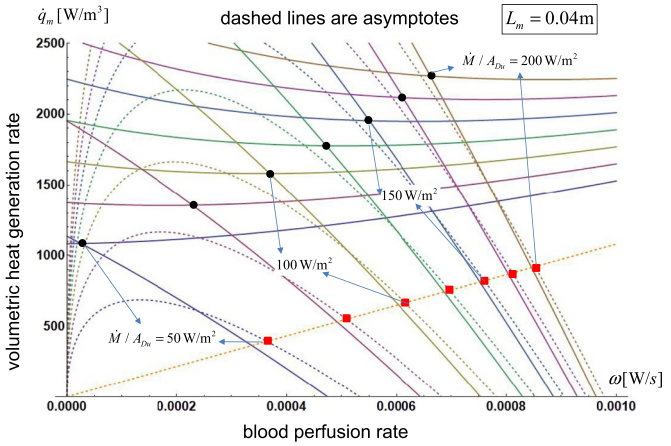

Fig. 11. The solutions of Eqs. (37) and (41) for small values of L_m (an example where asymptotic solution produces bad results).

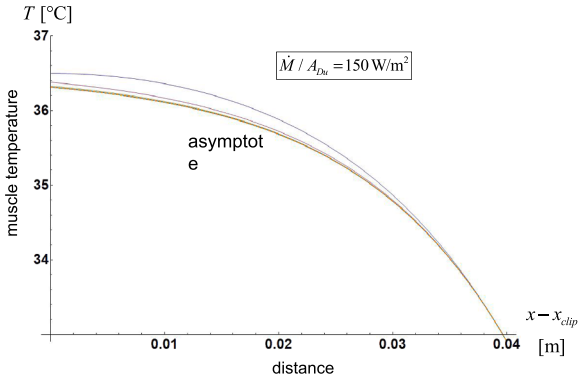

Fig. 12. Asymptotic behavior of temperature distribution near the skin surface.

4. Conclusions

It is important to note that the calculations of this study are based on two key theoretical foundations: the Pennes bioheat equation and the Fanger thermal comfort criteria. The results obtained in this study are valid only for the neutral conditions of thermal comfort under steady conditions. The limitations of the Pennes equation are worth mentioning. First, the temperature of the arterial blood is assumed to be constant when it travels from the heart to the capillary bed. As Kutz (2009) mentioned, small temperature variations occur only in blood vessels with diameters larger than 300 μm. The venous blood temperature is approximated by the local tissue temperature, and this is valid only for blood vessels with diameters smaller than 50 μm. Thus, without considering the thermal equilibration in the artery and vein in different vessel generations, the Pennes perfusion source term tends to overestimate the effect of blood perfusion. To accurately model the effect of blood perfusion, the temperature variation along the artery, and the heat recovered by the countercurrent vein must be accounted for.

Another issue is the spatial uniformity of the volumetric heat generation rate ($\dot{q}_m$) and the blood perfusion (ω). In general, it is probable that heat generation and blood perfusion are spatially distributed, even under steady conditions. Given that we assumed single values for these quantities, the results should be interpreted accordingly. The solution represents the general tendency "*on average, over a human body space, under steady conditions*." It should be noted that the Fanger thermal comfort model is a one-node model, and it is the foundation of the calculations in this study. From a mathematical point of view, if the distribution of the volumetric metabolic rate and blood perfusion are known a priori, it may still be possible to solve the governing equation, Eq. (24).

As we adopted simple Pennes bioheat equation, other physiological parameters and thermoregulatory mechanisms of the human body except for blood perfusion and volumetric heat generation are not reflected. Neither are the body thermal signals considered. Within the limitations mentioned above, it is expected that our solutions are suitable as quick estimation equations. The explicit asymptotic solutions given in Eqs. (51), (52) and (54) will be particularly useful in determining the functional dependence of the blood perfusion and volumetric heat generation rate on the value of the activity level. The total metabolic rate $\dot{M}$ is a primary variable representing the human activity level and is the key independent variable in this study. This is also true for many calculations involving thermal comfort. In numerous calculations of human comfort and the design of air conditioning systems, the Fanger criterion is a starting point. This study can, therefore, contribute to a better understanding of the human body response in maintaining thermal comfort under changing activity levels and environmental conditions.

Acknowledgment

Funding: This work was supported by the 2017 Yeungnam University Research Grant.

References

Acharya, S., Gurung, D.B., Saxena, V.P., 2014. Human males and females body thermoregulation: perfusion effect analysis. J. Therm. Biol. 45, 30–36.
ANSI/ASHRAE Standard 55, 2004. - Thermal Environmental Conditions for Human Occupancy.
Arkin, H., Xu, L.X., Holmes, K.R., 1994. Thermal comfort models: a review and numerical investigation. IEEE Trans. Biomed. 41 (2), 1994–1997.
ASHRAE, 2009. ASHRAE Handbook (SI) – Fundamentals, Chapter 6, Psychrometrics. ASHRAE, Atlanta.
Bhowmik, A., Singh, R., Repaka, R., Mishra, S.C., 2013. Conventional and newly developed bioheat transport models in vascularized tissues: a review. J. Therm. Biol. 38, 107–125.
Cengel, Y.A., Boles, M.A., 2014. Thermodynamics: An Engineering Approach, 8th ed. McGraw Hill.
Çetingül, M.P., Herman, C., 2010. A heat transfer model of skin tissue for the detection of lesions: sensitivity analysis. Phys. Med. Biol. 55 (19), 5933–5951.
Chen, M.M., Holmes, K.U., 1980. Microvascular contributions in tissue heat transfer. Ann. N.Y. Acad. Sci. 335, 137–150.
Das, K., Mishra, S.C., 2014. Study of thermal behavior of a biological tissue: an equivalence of Pennes bioheat equation and Wulff continuum model. J. Therm. Biol. 45, 103–109.
Fanger, P.O., 1970. Thermal Comfort – Analysis and Applications in Environmental Engineering. Danish Technical Press, Copenhagen.
Frank, S.M., Raja, S.N., Bulcao, C.F., Goldstein, D.S., 1999. Relative contribution of core and cutaneous temperatures, Downloaded from 〈www.physiology.org/journal/jappl〉 downloaded on 26 April 2018.
Incropera, F.P., DeWitt, D.P., Bergman, T.L., Lavine, S.A., 2012. Fundamentals of Heat and Mass Transfer. Wiley.
ISO 7730, 2005. Ergonomics of the thermal environment – Analytical determination and interpretation of thermal comfort using calculation of the PMV and PPD indices and local thermal comfort criteria.
Jović, S., Arsić, N., Vilimonović, J., Petković, D., 2016. Thermal sensation prediction by soft computing methodology. J. Therm. Biol. 62, 106–108.
Khiavi, N.M., Mehdi Maerefat, M., Seyed Alireza Zolfaghari, S.A., 2018. A new local thermal bioheat model for predicting the temperature of skin thermoreceptors of individual body tissues. J. Therm. Biol. 74, 290–302.
Klinger, H.G., 1974. Heat transfer in perfused biological tissue-I: general theory. Bull. Math. Biol. 36, 403–415.
Kutz, M., 2009. Biomedical Engineering and Design Handbook, Volume I: Biomedical Engineering Fundamentals, 2nd edition. McGraw-Hill Companies, Inc.
Mathematica, 2011. version 8, Wolfram.
McCutchan, J.W., Taylor, C.L., 1951. Respitory heat exchange with varying temperature and humidity of inspired air. J., Appl. Physiol. 4, 121–135.
Mitchell, J.W., Braun, J.E., 2012. Principles of Heating, Ventilation, and Air Conditioning in Buildings. Wiley.
Mitchell, J.W., Myers, G.E., 1968. An analytical model of the countercurrent heat exchange phenomena. Biophys. J. 897–911.
Moran, M.J., Shapiro, H.N., 2014. Moran Fundamentals of Thermodynamics, 8th ed. Wiley.
Pennes, H.H., 1948. Analysis of tissue and arterial Blood temperatures in the resting human forearm. J. Appl. Physiol. 1, 93–122.
Salloum, M., Ghaddar, N., Ghali, K., 2007. A new transient bioheat model of the human body and its integration to clothing models. Int. J. Therm. Sci. 46, 371–384.
Shrivastava, D., Subhash, C., Mishra, S.C., Christopher, J., Gordon, C.J., 2016. Modeling bioheat transfer processes and thermoregulatory responses. J. Therm. Biol. 62, 97.
Wang, Z., Ning, H., Ji, Y., Hou, J., He, Y., 2015. Human thermal physiological and psychological responses under different heating environments. J. Therm. Biol. 52, 177–186.
Weinhaum, S., Jiji, L.M., 1985. A new simplified equation for the effect of blood flow on local average tissue temperature. ASME J. Biomech. Eng. 107, 131–139.
Wulff, W., 1974. The Energy Conservation Equation for Living Tissue, IEEE Transactions of Biomedical Engineering, BME-21, 494-495.
Zhou, X., Xionga, J., Lian, Z., 2017. Predication of skin temperature and thermal comfort under two-way transient environments. J. Therm. Biol. 70, 15–20.
Zolfaghari, A., Maerefat, M., 2010. A new simplified thermoregulatory bioheat model for evaluating thermal response of the human body to transient environments. Build. Environ. 45, 2068–2076.

Jure Marn is currently teaching Power and Process Engineering subjects at Faculty for Mechanical Engineering at University of Maribor, Slovenia. His interests include heat and mass transfer in multi-phase system, non-Newtonian flows, and heat and mass transfer in bio-applications. He enjoys experimental and numerical work on the subject, and is strong proponent of the idea that way of solving the equations, be it via physical, or numerical experiments is not really important as long as foundations are strong, logical, and sufficiently explained. He finished undergraduate education at University of Maribor, and graduate education at University of Ljubljana, Slovenia as well as University of California at Los Angeles.

Mo Chung is a professor in the department of mechanical engineering Yeungnam University, Korea. He received BS and MS in mechanical engineering from Seoul National University, and Ph.D. from UCLA. He worked for Hyundai Motor Company and Korea Institute of Energy Research before he started teaching at Yeungnam University. His teaching subjects include thermodynamics, heat transfer, fluid mechanics, and applied mathematics. His research fields are building energy, smart energy, modeling and simulation of thermal systems, HVAC, and renewable energies. He was spending a Sabbatical Leave at University of Maribor at the time of the submission of this paper.

Dr. Jurij Iljaž received his Ph.D. in mechanical engineering (2012) from the University of Maribor, Faculty of mechanical engineering, where he is working now as researcher and assistant in the field of numerical modeling, CFD, thermodynamics, fluid mechanics and heat transfer. The field of his research work is solving inverse heat transfer problems, which he successfully applied to the diagnostic field in medicine, estimating the skin tumor parameters based on dynamic thermography.